CHEMICAL AND PROCESS ENGINEERING
29, 233–248 (2008)

MARCIN LEMAŃSKI, MICHAŁ KARCZ

PERFORMANCE OF LIGNITE-SYNGAS OPERATED TUBULAR SOLID OXIDE FUEL CELL

Institute of Fluid Flow Machinery Polish Academy Sciences, Gdańsk

Results of computations of a single fuel cell tube fuelled with lignite-derived synthesis gas have been presented. Gasifier reactions have been modelled as well as raw syngas pre-processing in pre-reformer to obtain fuel at a suitable steam-to-carbon ratio. The model employed in the analysis can cope with arbitrary mixture of hydrogen, steam, carbon monoxide, carbon dioxide and methane. Calculations have been conducted for various steam-to-air ratios in the gasifier.

Przedstawiono wyniki obliczeń pojedynczej rurki ogniwa paliwowego zasilanego gazem syntezowym uzyskanym w procesie gazyfikacji węgla brunatnego. Modelowano zarówno reakcje zachodzące w gazyfikatorze, jak i proces przygotowania paliwa do utylizacji w ogniwie paliwowym. Do analizy numerycznej wykorzystano opracowany wcześniej model, który umożliwia obliczanie parametrów ogniwa zasilanego dowolną mieszaniną wodoru, pary wodnej, tlenku węgla, dwutlenku węgla i metanu. Analizę prowadzono dla różnego stosunku pary wodnej i powietrza służącego do gazyfikacji węgla brunatnego.

1. INTRODUCTION

Both anthracite and lignite coal seem to be a main fuel in Poland in the past as for the upcoming years because its reserves are abundant. About 65 million tons of lignite are mined per year, that feed a power plants producing almost 35% of electric energy nationally [1]. However, the efficiency and the pollutant emission levels of conventional power plants are strongly disappointing. For these reasons, some advanced coal conversion technologies are still needed to enhance the way of the energy utilization. One of possible solutions is employment of coal gasification, i.e. a process between solid fuel and a reacting medium like air or steam, resulting in generation of syngas, which is a more flexible form of fuel for further processing [2]. Lignite has a great potential to be a source of synthesis gas that can be directly utilized either in boilers, gas turbine combustion chambers or solid oxide fuel cells (SOFC). It is believed that SOFC should perform well with gasification [3]. Electrochemical oxidation of hydrogen and carbon monoxide, being generally main constituents of syngas, in fuel cells is a relatively clean, reliable and efficient way of energy conversion when comparing to the conventional combustion. Especially an extremely low level of NO_x (less than 1 ppm) formation has been reported [4]. A pressurized SOFC can also be employed as

a part of high-efficient (50–70%) hybrid cycles with a gas turbine [5, 6]. SOFCs seem to be most advanced devices for low-power installations (up to 2 MW [7]) suitable for employing in the modern distributed power generation systems.

The problems of syngas utilization in SOFCs have been widely discussed. Gemmen and Trembly [8] presented the transport model in porous media suitable for multi-component synthesis gas. Carbon monoxide and hydrogen electro-kinetics and methane reforming kinetics they also discussed in the paper together with carbon deposition assessment. Some experimental and numerical results concerning SOFC operating with syngas fuel are presented by Suwanwarangkul et al. [9]. Also the electrochemical reaction rate ratio H_2:CO has been discussed in the paper. Experimental results concern the problem of fuel dilution at the anode side and the fuel composition, i.e. influence of the CO content on carbon deposition rate. In other paper of the same scientific centre [10], the numerical simulation of cathode-supported tubular SOFC operating with syngas from biomass gasification has been described. The differences between performances of humidified hydrogen- and syngas operated fuel cells have been presented in the paper. An analysis of a SOFC fuelled with biomass derived synthesis gas has also been presented by Cordiner et al. [11]. A commercial code Fluent coupled with external model to cope with electrochemical reactions has been employed for CFD calculations whereas 0D equilibrium approach has been used for gasifier modelling. The fuel cell efficiency for syngas has been estimated as equal to 34%. The problems of cogeneration cycle with SOFC, gas and steam turbines using coal gasification have been presented by Ghosh and De [3]. The feasibility study of high-temperature fuel cell combined with coal gasification system of a large output has been given by Kivisaari et al. [2]. They have shown that it is possible to obtain electricity from coal after gasification and further electrochemical processing in fuel cells with the electrical efficiency exceeding 40%.

In the present study, two numerical approaches have been considered: zero-dimensional modelling level, mainly for gasification process and fuel pre-processing prediction, and two-dimensional level for estimation of a tubular SOFC performance. These approaches are sometimes called system and mechanistic models, respectively [12]. For the former one an in-house code COM-GAS has been employed [13]. In the latter approach, a commercial code Fluent enhanced with own sub-procedures to cope with SOFC electrochemical processes have been used [14]. The possibility of efficient lignite utilization by means of electrochemical conversion in SOFC has been discussed.

2. METHODS OF COMPUTATION

2.1. GASIFICATION AND SYNGAS PREPROCESSING

Various organic feeds such as coal, wood, peat, oil residues, municipal waste and agriculture residues may be gasified as the primary fuel. Biomass gasification is of

special interest due to carbon dioxide neutrality [15]. Lignite composition employed in the present analysis (Table 1) has been taken from [16] as a real data from one of Polish mines.

Table 1. Selected lignite composition [16]

Component	Mass fraction [%]
C	66.00
H	5.53
O	26.25
N	1.00
S	1.22

An in-house code COM-GAS with gasification module has been employed for 0D calculations. The code was initially dedicated for advanced steam and gas turbine cycles analysis [13]. However, it can also cope with steam reforming and water-gas shift reactions in the reformer of the SOFC, as well as electrochemical reactions occurring at the SOFC electrodes [17]. One of the advantages of the code is a possibility of modelling of gasification process via Deringer's method. Implemented Deringer's model combined with the Gumz extension for sulphides has been fully described in [18, 13]. The algorithm involves the following reactions:

$$\mathrm{C} + \mathrm{CO_2} \rightarrow 2\mathrm{CO} \tag{1}$$

$$\mathrm{C} + \mathrm{H_2O} \rightarrow \mathrm{H_2} + \mathrm{CO} \tag{2}$$

$$\mathrm{C} + 2\mathrm{H_2} \rightarrow \mathrm{CH_4} \tag{3}$$

$$\mathrm{CO_2} + 2\mathrm{H_2} \rightarrow \mathrm{CO} + \mathrm{H_2O} \tag{4}$$

$$\frac{1}{2}\mathrm{S_2} + \mathrm{H_2} \rightarrow \mathrm{H_2S} \tag{5}$$

$$\frac{1}{2}\mathrm{S_2} + \mathrm{CO} \rightarrow \mathrm{COS} \tag{6}$$

Gasification is conducted with an addition of air-steam mixture. Steam fraction can be represented by the steam-to-air ratio β_{steam} defined as:

$$\beta_{\mathrm{steam}} = \frac{\dot{m}_{\mathrm{steam}}}{\dot{m}_{\mathrm{dry.air}}} \frac{M_{\mathrm{dry\ air}}}{M_{\mathrm{steam}}} \tag{7}$$

The gasification process has been considered under atmospheric pressure for various values of β_{steam} with constant raw syngas mass flow rate at the gasifier exit. Air and steam have been delivered at the temperature $t_{\mathrm{dry\ air}}$ = 20 °C and t_{steam} = 127 °C.

The raw syngas mixture after gasification process consisted mostly of hydrogen and carbon monoxide, balanced with nitrogen.

2.2. GASIFICATION AND SYNGAS PREPROCESSING

Stringent limit is required for fuel sulphur content in the feeding gas [11]. Some coolers, filters, and sulphur removal units (SRU) should be then included after gasifier to provide a clean fuel for SOFC [3]. The process is complicated but, on the other hand, syngas cleanup seems to be always more effective than conventional treatment after combustion due to much lower mass flow rate of fuel than that of exhaust gases [3, 8]. A lot of contaminants are present in raw syngas such as carbonyl sulphide COS or hydrogen sulphide H_2S being not fully tolerated by the fuel cell. Sulphur removal is usually carried out by multi-stage process involving gas cooling, COS hydrolysis over platinum-based catalyst according to the reaction:

$$\mathrm{COS} + \mathrm{H_2O} \rightarrow \mathrm{H_2S} + \mathrm{CO_2} \tag{8}$$

and subsequent reduction of H_2S to sulphur through absorption and oxidation in a tin bed. Final gas cleaning proceeds in ZnO bed [2]. It has been assumed in the present analysis that simplified fuel cleanup process is conducted without any pressure losses ($\Delta p = 0$) and at constant temperature $t = 400$ °C.

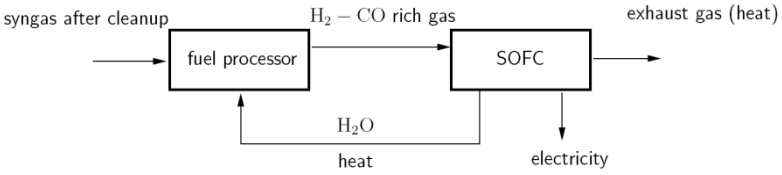

Fig. 1. Simple fuel cell system [20]

In the next step, the was directed for further processing according to a scheme shown in Fig. 1 to obtain fuel at suitable steam-to-carbon ratio S/C from the range of 1.5 to 3.0. In the present calculations, S/C = 1.8 has been assumed, similarly as in the paper by Campanari and Iora [19]. Details of the process modelling have been described in the paper by Badur and Lemański [17]. The fuel processor was fed directly by hydrocarbon fuel that could be either natural or synthesis gas. A recirculation of anode exhaust hot gases of high water content to the fuel processor leads to an enhancement of steam reforming or water-gas shift processes [17, 20]. As a result, a hydrogen- and carbon monoxide rich gas is being obtained. Due to electrochemical reactions inside the fuel cell, heat and electricity are simultaneously produced.

The whole system presented in Fig 1, together with a gasifier, has been calculated via 0D model. A single SOFC unit has been computed by means of 3D CFD code with boundary conditions directly taken from 0D analysis.

2.3. FUEL CELL MODEL

The details of the sub-model employed as an extension of commercial CFD code have been described elsewhere [21, 22]. The model has been developed subsequently and in the present version it can cope with:

- fuel as an arbitrary mixture of H_2, CO, CO_2, H_2O, CH_4, N_2,
- multi-component transport model including the Knudsen diffusion,
- electrochemical oxidation of both hydrogen and carbon monoxide,
- methane-steam reforming and water-gas shift reactions,
- exchange and limiting current density estimation.

The model is valid for 2D and 3D geometries of SOFC of either tubular or planar configuration. For the present analysis, the tubular fuel cell configuration (Fig. 2) has been assumed [21, 22]. Such a configuration is based on the Siemens–Westinghouse concept with cathode supported cell (L = 1.5 m) [5].

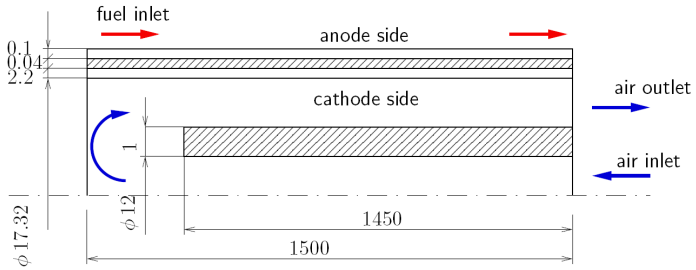

Fig. 2. Simplified geometry of tubular solid oxide fuel cell with characteristic dimensions as in [19]

Main components of tubular fuel cells are: rather thin electronic conductive anode usually made from Ni-YSZ cermet, oxygen-ion conductive layer of an electrolyte which is dense YSZ, and a thick cathode fabricated using $LaSrMnO_3$ [5, 6]. The cathode has also a high conductivity.

The anode composition and high temperature of cell operation cause that it is possible to perform internal reforming directly at a fuel electrode. However, an initial fuel pre-processing is still necessary due to some limits connected with carbon deposition leading to deterioration of the cell operation because of rapid increase of concentration polarization. The fuel temperature and compositions for various steam-to-air ratios β_{steam} in a gasifier have been assumed as boundary conditions for CFD calculations for a single tubular fuel cell. Fuel and air utilization factors have been assumed [19] as U_f = 0.69 and U_a = 0.175, respectively. These coefficients combined with assumed current density i_{avg} = 1780 A/m^2 are responsible for proper estimation of air and fuel mass flow rates at the cell inlet [21, 22]. Effective diffusivities of the species have been calculated based on the mean pore transport model [23] with binary diffusivities taken directly from the paper by Juan and Sunden [24] and Suwanwarangkul et al. [9].

Important parameters related to the structural nature of electrodes are porosity $\varepsilon = 0.5$, tortuosity $\tau = 3.0$, and mean pore radii $\bar{r} = 1.0$ μm. The same values were incorporated in the previous author's analysis [22]. Additionally the permeability of electrodes has been determined by Kozeny-Carman relationship [25]:

$$B = \frac{\varepsilon^2}{72\tau(1-\varepsilon)^2}(2\bar{r})^2 \tag{9}$$

Two main chemical and two electrochemical reactions may occur at the anode side of a fuel cell, namely methane reforming, water-gas shift reaction and electrochemical oxidation of hydrogen and carbon monoxide. The methane reforming reaction is as follows:

$$CH_4 + H_2O \rightarrow 3H_2 + CO \tag{10}$$

Endothermic reforming reaction usually leads to rapid cooling of the fuel entrance area [19, 22]. Due to rather low methane concentration in the syngas from lignite gasification, the reforming reaction has a little thermal impact on the cell. Water-gas shift reaction converting carbon monoxide and steam into hydrogen and carbon dioxide has a form:

$$CO + H_2O \rightarrow CO_2 + H_2 \tag{11}$$

Rates of formation of species or destruction for methane reforming (Eq. (10)) and water-gas shift (Eq. (11)) reactions can be calculated with the relationships given by Lehnert et al. [26]. Electrochemical oxidation of hydrogen is the basic reaction of solid-oxide type of fuel cell, where oxygen ions diffuse through the electrolyte from the cathode to anode side:

$$H_2 + O^{2-} \rightarrow H_2O + 2e^- \tag{12}$$

Similarly carbon monoxide, which is one of the main component of syngas and one of the product of reforming process (10), can be theoretically converted at anode via following reaction:

$$CO + O^{2-} \rightarrow CO_2 + 2e^- \tag{13}$$

The question is whether this reaction should be taken into account, because the water-gas shift reaction (Eq. (11)) is very fast comparing with electrochemical reaction (13), and whole carbon monoxide in the system may be converted into hydrogen. Only few papers explicitly give an information about the electrochemical H_2 to CO oxidation rate ratio. It has been shown [22] that CO electrochemical oxidation could slightly lower voltage generation in the cell. However, for the sake of simplicity, it has been assumed that CO is converted only via reaction (11), thus electricity is entirely produced from electrochemical oxidation of hydrogen and the theoretical voltage generated in an atmospheric fuel cell can be estimated from the classical Nernst equation [3, 4, 6, 27, 28]:

$$\Delta E = \frac{-\Delta G^0_{\mathrm{H_2O}}}{2\mathrm{F}} + \frac{RT}{2F}\ln\frac{X_{\mathrm{H_2}} X^{1/2}_{\mathrm{O_2}}}{X_{\mathrm{H_2O}}} \tag{14}$$

Real operating voltage is however lower than the value calculated via Eq. (14) due to fuel cell polarizations. Ohmic losses η_{ohm} due to electronic and ionic resistivities of fuel cell elements are especially important at lower operating temperature in electrolyte. Conductivities are estimated from temperature dependent closures separately for every fuel cell element [19]. Activation losses η_{act} are connected with the energy barrier for initialisation of electrochemical reaction (12) and can be estimated implicitly from the Butler–Volmer equation [4, 28]:

$$i = i_0 \mathrm{e}^{(1-\alpha) f \eta_{\mathrm{act}}} - i_0 \mathrm{e}^{-\alpha f \eta_{\mathrm{act}}} \tag{15}$$

where α is a symmetry factor commonly assumed to be 0.5 for fuel cells, and f is defined as:

$$f = \frac{F}{RT} \tag{16}$$

Rather straightforward way is to calculate these polarizations explicitly from hyperbolic sine approximation of the Butler–Volmer equation [27]:

$$\eta_{\mathrm{act}} = \frac{2}{nf}\sinh^{-1}\left(\frac{i}{i_0}\right) \tag{17}$$

where n is the number of electrons transferred due to elementary electrochemical reaction (12). Concentration polarizations η_{conc} are important for high current density and high fuel utilization rates because of the fuel dilution and the problem of reactions substrates and products transport from and to the electrodes. These can be estimated from [12]:

$$\eta_{\mathrm{conc}} = \frac{1}{nf}\ln\left(1 - \frac{i}{i_L}\right) \tag{18}$$

The values of exchange i_0 and limiting i_{L} current densities have been calculated based on the relationships given by Campanari and Iora [19]. The implemented model has been verified against experimental and numerical data for humidified hydrogen and natural gas fuelled tubular fuel cells. Details one can find elsewhere [21, 22].

3. COMPUTATIONS

3.1. ESTIMATION OF SYNGAS COMPOSITION

Mole fractions of raw syngas constituents obtained from lignite for various β_{steam} values are shown in Fig. 3. The resulting syngas temperature is presented in Fig. 4.

The gasifier exhaust temperature varies upon the β_{steam} ratio. The maximum of temperature t = 880 °C occurs at β_{steam} = 0.3 for O/C = 0.4 (oxygen mole fraction/carbon mole fraction) ratio at the fuel cell inlet, the values being close to t = 927 °C and O/C < 0.4 recommended by Prins et al. [15] for efficient fuel gasification under atmospheric pressure.

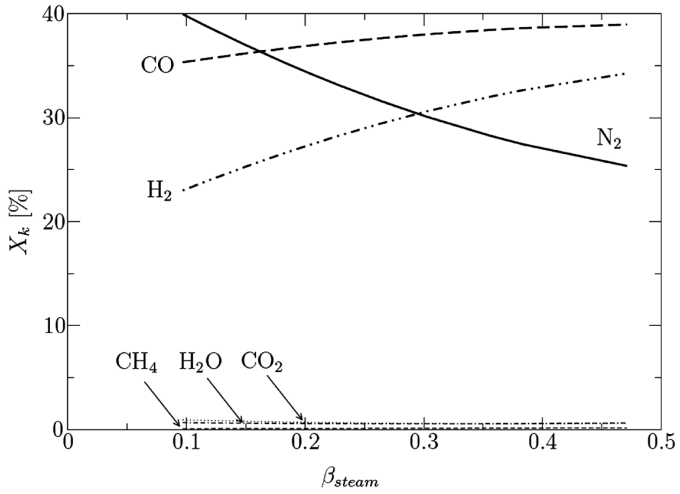

Fig. 3. Change of mole fraction of raw syngas components with the steam-to-air ratio β_{steam}

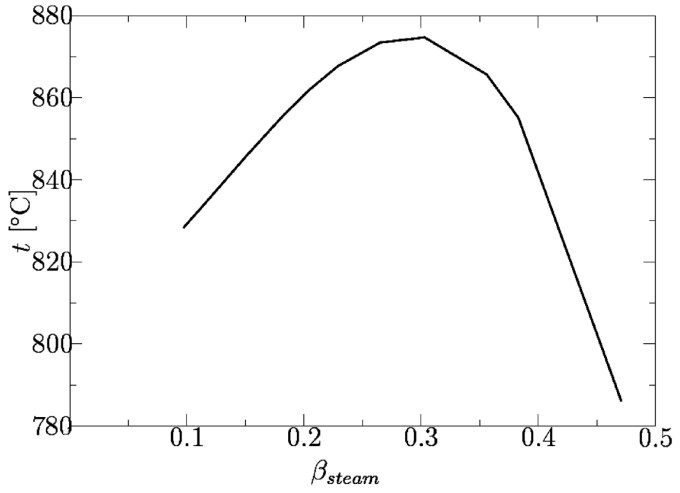

Fig. 4. Raw syngas temperature change at gasifier exit

The mole fractions of hydrogen and carbon monoxide presented in Fig. 3 are similar to those presented in [15] for gasification under equilibrium conditions at t = 877 °C. The only differences are for steam and carbon dioxide mole fractions

which are much lower in current analysis than 10% reported for the biomass derived syngas in [15]. In the paper by Suwanwarangkul et al. [9] different syngas fuels have been considered. For syngas with the following composition: X_{H2} = 20%, X_{H2O} = 3%, X_{CO} = 20%, X_{CO2} = 0% and X_{N2} = 57%, close to that presented in Fig. 3, they reported very good fuel cell performance, even comparable with humidified hydrogen, pointing to the possibility that carbon monoxide should be a useful fuel for SOFC.

The raw synthesis gas from lignite gasification is hydrogen- and carbon monoxide rich. The mixture contains only small amounts of methane and steam (below 1%). Due to small H_2O content there is a need of further post-processing in fuel cell pre-reformer to obtain higher steam-to-carbon ratio S/C. The gas cleanup should be also proceeded to eliminate COS and H_2S from the mixture.

Table 2. Syngas compositions at the anode inlet (mole fraction [%])

β_{steam}	H_2O	CO_2	N_2	H_2	CO	CH_4
0.10	18.210	26.210	39.881	5.610	10.080	0.009
0.12	18.760	26.180	38.731	5.930	10.390	0.010
0.21	20.840	26.080	34.178	7.310	11.580	0.012
0.30	22.740	26.030	30.026	8.600	12.590	0.014
0.47	24.860	25.850	25.299	10.220	13.750	0.021

The resulting compositions are given in the Table 2 as functions of β_{steam}. These values have been finally adopted for the CFD analysis of a tubular fuel cell.

3.2. MODELLING OF A FUEL CELL PERFORMANCE

The presented SOFC model has been implemented into commercial CFD code Fluent [14] by means of user-defined subroutines. Similarly as in papers [21, 22], ideal gas mixture, incompressible and laminar flow, homogeneous and isotropic nature of electrodes have been assumed. Because of strong temperature dependence of fuel cell performance, heat radiation should be also incorporated in the model [7]. However, for the sake of simplicity and under the assumption that the fuel cell tube operates in the bunch of identical tubes with uniform thermal conditions, no radiative heat transfer has been considered in the present study. Fuel cell geometry presented in Fig. 2 has been discretized by means of finite volume method (FVM). The density of the grid has been assumed based on sensitivity studies. Especially regions near active electrode and electrolyte interfaces should be treated carefully. Number of the computational cells reaches 17 000 only because of simplified two-dimensional axisymmetric domain. However, the computational time has been relatively long due to implementation of additional charge balance and species transport equations. An analysis has been conducted for all compositions given in Table 2. The results are presented as a change of general fuel cell parameters with gasification process steam-to-air ratio β_{steam}.

Two types of analysis have been performed, i.e. with a constant current density and variable mass flow rate of fuel at the anode, and with a constant mass flow rate of fuel and variable current density.

3.3. CONSTANT CURRENT DENSITY CASE

The distribution of species along the anode channel is presented in Fig. 5 for β_{steam} = 0.10 and i_{avg} = 1780 A/m^2. The predicted fuel constituent changes are obvious because of continuous consumption of hydrogen and carbon monoxide via electrochemical oxidation (Eq. (12)) and water-gas shift reaction (Eq. (11)), respectively.

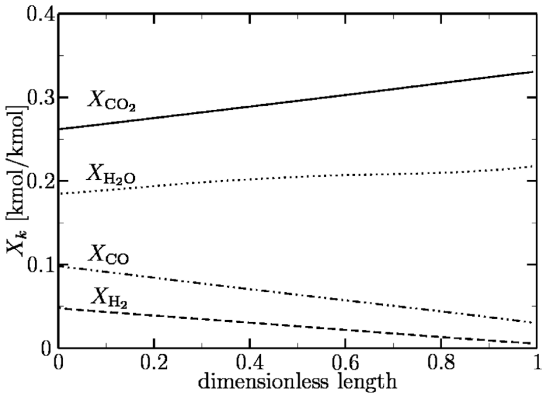

Fig. 5. Distribution of species at the anode (β_{steam} = 0.1)

Lack of methane at the anode side (X_{CH_4} < 0.1%) causes main differences between syngas and natural gas operated fuel cells. In the present case, reforming reaction (10) did not occur, so no hydrogen has been produced at the cell entrance area due to methane conversion [22]. Continuous carbon monoxide conversion at the anode side results however in hydrogen production. Slope of the hydrogen mole fraction X_{H_2} curve is then less pronounced in Fig 5. Similar results have been presented in the paper by Suwanwarangkul et al. [10] for synthesis gas with similar composition.

Main fuel cell parameters for various steam-to-air ratios β_{steam} and constant average current density across the cell are presented in Fig. 6. The increment of voltage, power and efficiency are rather small. There is evident anode average temperature growth with increasing β_{steam}. However, the estimated average temperature value seems to be slightly too high for syngas fuel as reported in [10]. This could be an effect of initial assumption that radiative heat transfer is not considered in the present computations. The problem could be especially important for the modelling of heat transfer between air inducing tube and the main cell structure [7].

The fuel cell efficiency η, nearly constant and equal to 0.33 (Fig. 6) is very close to the values η = 0.34 reported by Cordiner et al. [11] and η = 0.36 presented by Suwanwarangkul et al. [10] for the biomass derived syngas. Slight changes of main parame-

ters are connected with changes of the mass flow rate for various fuel compositions at the anode inlet due to dependence:

$$\dot{m}_f = \frac{i_{\text{avg}} A_{\text{cell}}}{2FU_f} \frac{\bar{M}}{\left(X_{\text{H}_2} + X_{\text{CO}} + 4X_{\text{CH}_4}\right)} \tag{19}$$

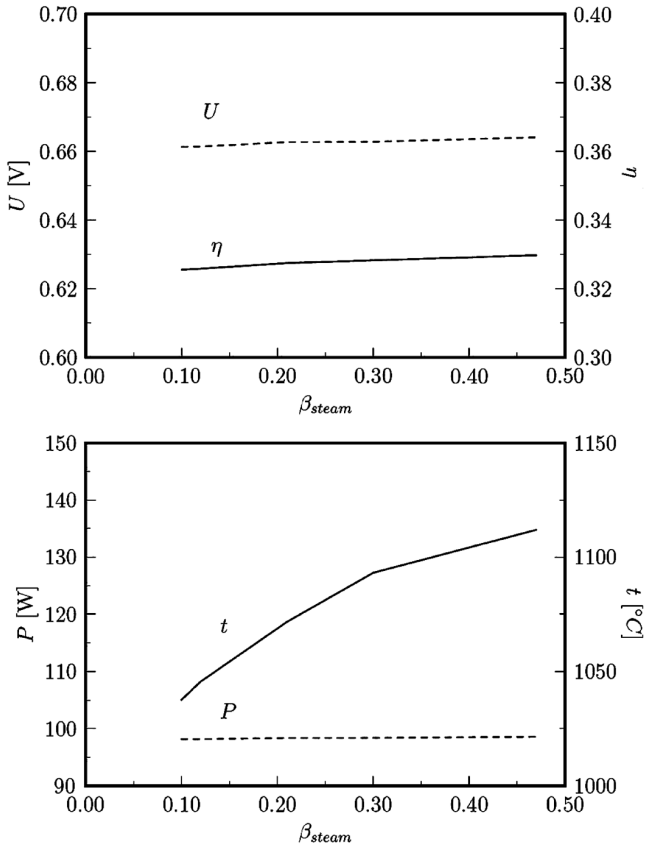

Fig. 6. Dependence of general fuel cell performance on the steam-to-air ratio β_{steam} for constant average current density case

Relevant airflow changes at the cathode inlet have been evaluated based on the oxygen requirement for the hydrogen oxidation via Eq. (12) considering air utilization factor U_{a} [3].

3.4. CONSTANT FUEL MASS FLOW RATE CASE

In the next step, a constant fuel mass flow rate analysis has been conducted. The general fuel cell behaviour for various β_{steam} is presented in Fig. 7.

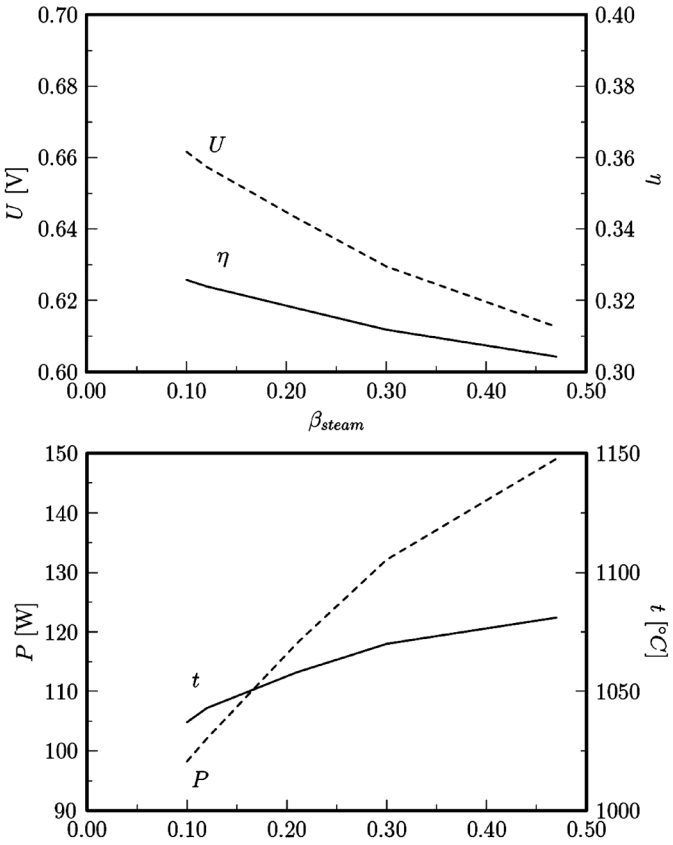

Fig. 7. Dependence of a general fuel cell performance on the steam-to-air ratio β_{steam} for a constant fuel mass flow rate case

The value of $\dot{m}_f = 2.05 \cdot 10^{-4}$ kg/s has been taken from the previous computations with a constant current density i_{avg} for the steam-to-air ratio $\beta_{\text{steam}} = 0.10$. Contrary to the results presented in Fig. 6 for i_{avg} = const, in the present case of $\dot{m}_f$ = const a strong parameter dependence on β_{steam} occurs. Decreasing voltage and efficiency followed a simultaneous power and temperature increase. Changes are more pronounced for lower steam-to-air ratio values and tend to reach some limit at high β_{steam}. The current density also changes with the steam-to-air ratio (Fig. 8).

The current density increment results in simultaneous voltage lowering due to increase of activation and concentration polarizations according to Eqs. (17) and (18), respectively. Also the temperature increment lowers voltage generation due to strong dependence of the Gibbs free enthalpy $\Delta G^0_{\text{H}_2\text{O}}$ in Eq. (14) on temperature.

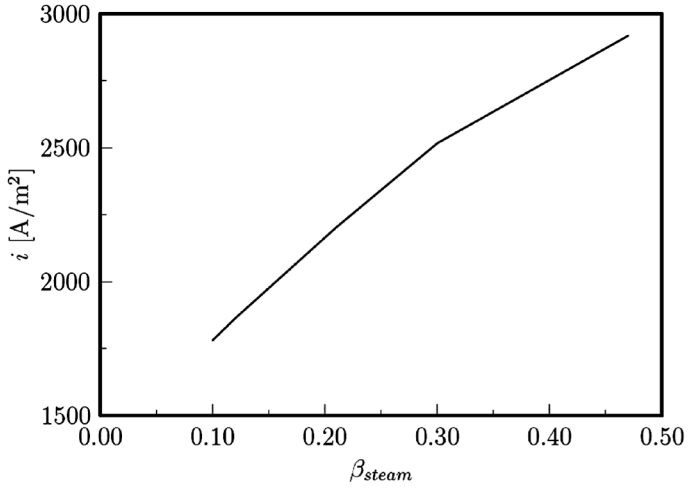

Fig. 8. Dependence of the current density on the steam-to-air ratio β_{steam} for a constant fuel mass flow rate case

It is possible to utilize lignite coal in fuel cells via gasification process which allows one to convert solid fuels into the synthesis gas. It needs however some raw gas pre-processing in a cleanup systems and use of pre-reformers. The results are rather encouraging with the efficiency above 30% for a single fuel cell. It is believed that in the case of hybrid cycles with fuel cells, the efficiency could be considerably higher. As far as the synthesis gas contains a remarkable fraction of carbon monoxide, there is a strong need of detailed analysis on CO electrochemistry that competes with water-gas shift reaction and H_2 electrochemistry at the anode. The integral temperature at the anode seems to be slightly too high for synthesis gas operated fuel cell. The radiative heat transfer should be included in the further analysis to asses a real influence of those phenomena on a fuel cell performance.

ACKNOWLEDGEMENTS

The authors would like to express their gratitude to Prof. J. Badur for his ideas and support on this work. This research has been supported by the State Committee of Scientific Research (KBN) under the contract 3T10B 05026.

SYMBOLS

A – area, m^2
B – permeability, m^2/s
D – diffusivity coefficient, m^2/s
F – Faraday constant, C/mol
i – current density, A/m^2
$\dot{m}$ – mass flow rate, kg/s
M – molecular weight, kg/kmol
$\bar{M}$ – mean molecular weight, kg/kmol

p – pressure, Pa
R – gas constant, J/(mol·K)
t – temperature, °C
U – utilization factor (fuel, oxidizer)
X – mole fraction
ε – porosity factor
η – efficiency, voltage losses, V
τ – tortuosity factor

SUBSCRIPTS AND SUPERSCRIPTS

0 – standard, referential
act – activation
avg – average
conc – concentration
eff – effective
f – fuel
k – component of a mixture
ohm – ohmic

REFERENCES

[1] KOZŁOWSKI Z., Appl. Energ., 2003, 74, 323.
[2] KIVISAARI T., BJORNBOM P., SYLWAN C., JACQUINOT B., JANSEN D., DE GROOT A., Chem. Eng. J., 2004, 100, 167.
[3] GHOSH S., DE S., Energy, 2007, 31, 345.
[4] SANCHEZ D., CHACARTEGUI R., MUNOZ A., SANCHEZ T., J. Power Sources, 2006, 160, 1074.
[5] SINGHAL S.C., Solid State Ionics, 2000, 135, 305.
[6] KEE R.J., ZHU H., GOODWIN D.G., *Solid-oxide fuel cells with hydrocarbon fuels*, Proc. Combustion Institute, 2005, 30, 2379.
[7] SUWANWARANGKUL R., CROISET E., PRITZKER M.D., FOWLER M.W., DOUGLAS P.L., ENTCHEV E., J. Power Sources, 2006, 154, 74.
[8] GEMMEN R.S., TREMBLY J., J. Power Sources, 2000, 161, 1084.
[9] SUWANWARANGKUL R., CROISET E., ENTCHEV E., CHAROJROCHKUL S., PRITZKER M.D., FOWLER M.W., DOUGLAS P.L., CHEWATHANAKUP S., MAHAUDOM H., J. Power Sources, 2006, 161, 308.
[10] SUWANWARANGKUL R., CROISET E., PRITZKER M.D., FOWLER M.W., DOUGLAS P.L., ENTCHEV E., J. Power Sources, 2007, 166, 386.
[11] CORDINER S., FEOLA M., MULONE V., ROMANELLI F., Appl. Therm. Eng., 2007, 27, 738.
[12] BHARADWAJ A., ARCHER D.H., RUBIN E.S., ASME J. Fuel Cell Sci. Technol., 2005, 2, 38.
[13] TOPOLSKI J., *Diagnosis of combustion processes in a gas-steam cycles*. PhD Thesis, Inst. Fluid-Flow Machinery, Polish Academy of Sciences, Gdańsk, Poland, 2002 (in Polish).
[14] Fluent Inc., 2005.
[15] PRINS M.J., PTASINSKI K.J., JANSSEN F.J.J.G., Energy, 2007, 32, 1248.
[16] KRUCZEK S., 2001, *Boilers. Construction and analysis*, Technical University of Wrocław (in Polish).
[17] BADUR J., LEMAŃSKI M., Inż. Chem. Proc., 2005, 26, 157 (in Polish).
[18] KOZACZKA J., *Gasification processes. Engineering methods of calculations*, AGH Kraków, 1994 (in Polish).
[19] CAMPANARI S., IORA P., J. Power Sources, 2004, 132, 113.
[20] HAYNES C., WEPFER W.J., Energy Conversion Management, 2000, 41, 1123.
[21] KARCZ M., Inż. Chem. Proc., 2006, 27, 201 (in Polish).

[22] KARCZ M., Inż. Chem. Proc., 2007, 28, 307.
[23] YAKABE H., HISHINUMA M., URATANI M., MATSUZAKI Y., YASUDA I., J. Power Sources, 2000, 86, 423.
[24] YUAN J., SUNDEN B., ASME J. Fuel Cell Sci. Tech., 2006, 3, 89.
[25] Ni M., LEUNG M.K.H., LEUNG D.Y.C., J. Power Sources, 2006,163, 460.
[26] LEHNERT W., MEUSINGER J., THOM F., J. Power Sources, 2000, 87, 57.
[27] NOREN D.A., HOFFMAN M.A., J. Power Sources, 2005, 152, 175.
[28] ATKINS P.W., 2001, *Physical Chemistry*, PWN, Warszawa, (in Polish).

MARCIN LEMAŃSKI, MICHAŁ KARCZ

ANALIZA PRACY OGNIWA PALIWOWEGO ZASILANEGO GAZEM SYNTEZOWYM Z GAZYFIKACJI WĘGLA BRUNATNEGO

Przedstawiono wyniki obliczeń dla pojedynczej rurki ogniwa paliwowego SOFC zasilanego gazem syntezowym uzyskanym w procesie gazyfikacji węgla brunatnego. Na poziomie analizy zerowymiarowej modelowano podstawowe reakcje zachodzące w gazyfikatorze oraz proces dalszego przygotowania otrzymanego gazu syntezowego do utylizacji w ogniwie paliwowym. W trójwymiarowych obliczeniach numerycznych skorzystano z modelu, który umożliwia obliczanie ogniwa zasilanego dowolną mieszaniną wodoru, pary wodnej, tlenku węgla, dwutlenku węgla i metanu. Wykorzystano istniejące domknięcia na straty napięcia oraz właściwości materiałowe. Podobnie jak we wcześniejszych pracach zastosowano model wieloskładnikowy dyfuzji, współczynniki dyfuzji zaś zaczerpnięto z literatury. Założono, że w ogniwie występuje tylko elektrochemiczna reakcja utleniania wodoru, a tlenek węgla ulega konwersji chemicznej jedynie w reakcji gazu wodnego, której produktem jest wodór i dwutlenek węgla. Analizę numeryczną wykonano dla różnych wartości stosunku strumienia masowego pary wodnej i powietrza β_{steam}, a także dla stałej gęstości prądu oraz stałego strumienia masowego paliwa na wlocie do anody. Otrzymano charakterystyki pracy ogniwa dla różnych wartości β_{steam}. Zmiany charakterystycznych parametrów pracy ogniwa są bardziej wyraźne dla przypadku stałego strumienia paliwa, niż dla przypadku założonej stałej gęstości prądu. Dla obu wariantów uzyskano stosunkowo wysoką temperaturę pracy ogniwa, co tłumaczy się pominięciem w modelowaniu radiacyjnej wymiany ciepła. Obliczona sprawność ogniwa (33%) jest zgodna z danymi literaturowymi dla układów ogniw zasilanych gazem syntezowym z procesu gazyfikacji zarówno biomasy, jak i węgla.

Received 3 August 2007